Biological Chemistry ‘Just Accepted’ Papers

Biological Chemistry ‘Just Accepted’ Papers are papers published online, in advance of appearing in the print journal. They have been peer-reviewed, accepted and are online published in manuscript form, but have not been copy edited, typeset, or proofread. Copy editing may lead to small differences between the Just Accepted version and the final version. There may also be differences in the quality of the graphics. When papers do appear in print, they will be removed from this feature and grouped with other papers in an issue.

Biol Chem ‘Just Accepted’ Papers are citable; the online publication date is indicated on the Table of Contents page, and the article’s Digital Object Identifier (DOI), a unique identifier for intellectual property in the digital environment (e.g., 10.1515/hsz-2011-xxxx), is shown at the top margin of the title page. Once an article is published as **Biol Chem ‘Just Accepted’ Paper** (and before it is published in its final form), it should be cited in other articles by indicating author list, title and DOI.

After a paper is published in **Biol Chem ‘Just Accepted’ Paper** form, it proceeds through the normal production process, which includes copy editing, typesetting and proofreading. The edited paper is then published in its final form in a regular print and online issue of **Biol Chem.** At this time, the **Biol Chem ‘Just Accepted’ Paper** version is replaced on the journal Web site by the final version of the paper with the same DOI as the **Biol Chem ‘Just Accepted’ Paper version.**

Disclaimer

Biol Chem ‘Just Accepted’ Papers have undergone the complete peer-review process. However, none of the additional editorial preparation, which includes copy editing, typesetting and proofreading, has been performed. Therefore, there may be errors in articles published as **Biol Chem ‘Just Accepted’ Papers** that will be corrected in the final print and online version of the Journal. Any use of these articles is subject to the explicit understanding that the papers have not yet gone through the full quality control process prior to advanced publication.

Biological Chemistry **'Just Accepted' paper**
ISSN (online) 1437-4315
DOI: 10.1515/hsz-2016-0153

Research Article

Analysis of anticoagulants for blood-based quantitation of amyloid β oligomers in the sFIDA assay

Kateryna Kravchenko[1], Andreas Kulawik[1,2], Maren Hülsemann[1], Katja Kühbach[1], Christian Zafiu[1], Yvonne Herrmann[1], Christina Linnartz[1], Luriano Peters[1], Tuyen Bujnicki[1], Johannes Willbold[1], Oliver Bannach[1,2] and Dieter Willbold[1,2,*]

[1]ICS-6 Structural Biochemistry, Forschungszentrum Jülich, Wilhelm-Johnen-Str., D-52425 Jülich, Germany

[2]Institut für Physikalische Biologie, Heinrich-Heine-Universität Düsseldorf, Universitätsstraße 1, D-40225 Düsseldorf, Germany

*Corresponding author

e-mail: d.willbold@fz-juelich.de

Abstract

Early diagnostics at the preclinical stage of Alzheimer's disease is of utmost importance for drug development in clinical trials and prognostic guidance. Since soluble Aβ oligomers are considered to play a crucial role in the disease pathogenesis, several methods aim to quantify Aβ oligomers in body fluids such as cerebrospinal fluid (CSF) and blood plasma. The highly specific and sensitive method surface-based fluorescence intensity distribution analysis (sFIDA) has successfully been established for oligomer quantitation in CSF samples. In our study, we explored the sFIDA method for quantitative measurements of synthetic Aβ particles in blood plasma. For this purpose, EDTA, citrate and heparin treated blood plasma samples from five individual donors were spiked with Aβ coated silica nanoparticles (Aβ-SiNaPs) and were applied to the sFIDA assay. Based on the assay parameters linearity, coefficient of variation and limit of detection, we found that EDTA plasma yields the most suitable parameter values for quantitation of Aβ oligomers in sFIDA assay with a limit of detection of 16 fM.

Keywords: Alzheimer's disease diagnostic biomarkers; Amyloid beta oligomers; neurodegenerative diseases; blood plasma; sFIDA, silica nanoparticles.

Introduction

Alzheimer's disease (AD) is the most frequent form of dementia which affects more than 35 million people worldwide (Wimo *et al.*, 2013). Since age is considered to be the major risk factor for AD, the case number is expected to dramatically increase in the next decades as a consequence of the aging society. The clinical onset of AD is preceded by pathophysiological changes years before outbreak of the disease (Blennow, 2004). Early diagnostics at the preclinical stage of the disease is highly desired for drug development in clinical trials and prognostic guidance.

Major pathological hallmarks of AD are extracellular amyloid plaques consisting mainly of amyloid beta (Aβ) peptide as well as intracellular neurofibrillary tangles composed of tau protein (Selkoe, 1991). More recent data indicate that oligomeric Aβ is the most toxic species and is therefore of interest both as drug target and candidate biomarker (Haass and Selkoe, 2007; Blennow *et al.*, 2015).

On that account, we developed a highly sensitive oligomer-specific diagnostic assay designated surface-based fluorescence intensity distribution analysis (sFIDA) (Birkmann *et al.*, 2006; Birkmann *et al.*, 2007; Funke *et al.*, 2007; Funke *et al.*, 2010; Bannach *et al.*, 2012; Wang-Dietrich *et al.*, 2013; Kühbach *et al.*, 2016). In sFIDA, Aβ is captured to a functionalized glass surface by Aβ specific antibodies which recognize the N-terminus of the molecule. Subsequently, Aβ is decorated by two fluorescently labeled antibodies. Since the same or overlapping epitopes are recognized by both capture and detection antibodies, the assay is insensitive for monomeric Aβ which is omnipresent also in healthy subjects. Images from the surface are obtained using dual-color total internal reflection fluorescence microscopy (TIRFM). The number of colocalized pixels with signal intensities above background is referred to as sFIDA readout, which correlates with the number of Aβ oligomers in the sample. As a calibration standard in the sFIDA assay, 30 nm silica nanoparticles coated with $A\beta_{1\text{-}42}$ peptides (Aβ-SiNaPs) are used. Aβ-SiNaPs have been shown to be a suitable standard in Aβ oligomer quantitation due to their uniform size and defined number of accessible epitopes. Moreover, the particles are not prone to aggregation and are stable over several months (Hülsemann *et al.*, 2016).

sFIDA has been proven as a capable tool for the quantitation of Aβ oligomers from cerebrospinal fluid with a large sensitive range of detection. However, lumbar puncture,

though generally considered as safe, goes along with risks and is often experienced as uncomfortable for patients. Hence, the diagnosis from blood preparations after venipuncture is a worthwhile aim.

Blood can be processed either as serum or as plasma, which is the noncoagulated liquid component of blood after centrifugation. Coagulation is prevented by addition of anticoagulants of which EDTA, citrate, and heparin are the most commonly used in clinical practice (Jambunathan and Galande, 2014). EDTA and citrate prevent the formation of thrombin by chelating calcium required for the blood clotting cascade (Davie and Ratnoff, 1964), whereas heparin functions by activating antithrombin (Olson and Chuang, 2002).

The choice of anticoagulant for blood plasma preparation is an important factor in the preanalytical phase of assay development and can have a considerable effect on the identification of biomarkers as shown for a variety of assays concerning the detection of e.g. cytokines (Riches *et al.*, 1992), miRNA (Leidinger *et al.*, 2015), proteins (Banks *et al.*, 2005; Hsieh *et al.*, 2006), enzymes (Gerlach *et al.*, 2005), amino acid analysis (Parvy *et al.*, 1983; Hubbard *et al.*, 1988; Chuang *et al.*, 1998) and other analytes (Fendl *et al.*, 2016; Ribeiro *et al.*, 2016).

The goal of the present study was to compare the effect of different anticoagulants on the sFIDA assay and identify the most suitable anticoagulant regarding assay standardization. Therefore, a dilution series of Aβ-SiNaPs was spiked in blood plasma supplemented with different anticoagulants (EDTA, citrate and heparin, respectively) and were subsequently applied to the sFIDA assay. Based on the assay parameters linearity, coefficient of variance and limit of detection, the effect of the anticoagulants on the assay outcome was investigated.

Results

Aβ-SiNaPs were spiked in a log 10 dilution series to EDTA, citrate and heparin plasma, each of five individual healthy donors and subjected to sFIDA assay. As a preprocessing procedure all images underwent artifact detection. For Aβ-SiNaPs spiked in EDTA plasma, citrate plasma, heparin plasma and PBS 81.4%, 87.9%, 88.0% and 89.2% of the total number of images passed quality control, respectively.

Inspection of the images for sFIDA analysis revealed differences for the different anticoagulants (Figures 1 and 2). For channel 0 (em. 635 nm / exc. 705 nm) the major peak in intensity distribution for EDTA was approximately at 2400, for citrate at 1700 and for heparin at 900 on a 14-bit grayscale, and for channel 1 (em. 488 nm / exc. 525 nm) at approximately 1300, 1300 and 1000, respectively (Figure 2), as shown for blood plasma samples spiked in 1 pM Aβ-SiNaPs. This indicates that the overall intensity of images obtained from heparin treated blood plasma are considerably lower compared to EDTA and citrate, as can also be seen in representative images (Figure 1, left hand column). Furthermore, the variation in intensity distribution between the images is higher for heparin compared to EDTA and citrate plasma (Figure 1, middle and right hand column).

For deeper analysis, sFIDA readout was calculated which is the number of colocalized pixels above background. A correlation between Aβ-SiNaP concentration and sFIDA readout was observed from 100 pM down to the lowest concentration of 10 fM for all plasma samples (Figure 3). In order to further characterize the effect of different anticoagulants on the sFIDA readout of Aβ-SiNaP spiked plasma samples, the linearity of the data was assessed as well as the coefficient of variation (CV) as a criterion for intra-assay precision and limit of detection (LOD) as a criterion for assay sensitivity were calculated.

Linearity

The sFIDA assay is known to have a wide sensitive detection range for Aβ oligomers. However, the linearity of the assay's readout is influenced by a variety of factors. To investigate the impact of anticoagulants in blood plasma samples on the linearity of the sFIDA readout, the Pearson's correlation coefficient, Mandel's fitting test as well as Lack-of-fit test were calculated (Table 1).

Nearly ideal linear relationship in terms of Pearson's correlation of $\rho = 0.94$ was found for EDTA blood plasma and PBS diluents, whereas considerably lower values of $\rho = 0.37$ and $\rho = 0.64$ were obtained for dilutions in citrate and heparin blood plasma, respectively (table 2). Since Pearson's correlation coefficient ρ has very limited significance as a criterion for linearity, Mandel's fitting test as well as Lack-of-fit test for the first and second order calibration curve was performed which are recommended and well established methods for testing linearity (Van Loco *et al.*, 2002; Sanagi *et al.*, 2010). Likewise, Mandel's fitting test and Lack-of-fit test,respectively, indicate good linearity for EDTA plasma and PBS control,

whereas for citrate and heparin a second order calibration curve is the function preferred (Table 1).

Coefficient of variation

Coefficient of variation (CV) was calculated to assess intra-assay precision, which differs between the anticoagulants (Figure 4). The lowest mean CV of 28% was obtained for EDTA plasma followed by 39% for citrate plasma and 67% for heparin plasma. For PBS a CV of 51% was obtained.

Limit of detection

Limit of detection (LOD) was calculated to investigate the effect of different anticoagulants on assay sensitivity as the mean for five donors. As each donor was measured in six replicates, the mean LOD calculation is based on 30 negative controls. Significant differences in mean LOD for Aβ-SiNaP dilution series in EDTA, citrate and heparin plasma as well as in PBS were observed (Figure 5). The lowest mean LOD of 16 fM was obtained for Aβ-SiNaPs spiked in EDTA plasma followed by 19 fM (incl. outlier: 34 fM) for citrate, 27 fM for PBS and 34 fM (incl. outlier: 280 fM) for heparin. Additionally, the median LOD was calculated being more robust towards outliers as observed for citrate and heparin. In agreement with mean LOD the lowest median LOD of 16 fM was obtained for Aβ-SiNaP spiked in EDTA plasma followed by 22 fM for citrate plasma, 23 fM for PBS and 31 fM for heparin plasma (data not shown).

Summary

Mean Pearson's correlation coefficient between spiked Aβ-SiNaPs and sFIDA readout, mean CV [%] and mean LOD for all three anticoagulants and PBS are summarized in Table 2. Highest linearity, highest intra-assay precision and highest sensitivity of the sFIDA assay was obtained for Aβ-SiNaP-spiked EDTA plasma.

Discussion

The choice of anticoagulants for blood plasma preparation can have a significant impact on the detection of biomarkers. The aim of the present study was to compare the effect of different anticoagulants on the sFIDA readout and identify the most suitable anticoagulant

regarding assay standardization. For this purpose, a dilution series of Aβ-SiNaPs was spiked in human blood plasma samples supplemented with different anticoagulants (EDTA, citrate and heparine, respectively) and was subsequently applied to the sFIDA assay. The assay outcome was evaluated by means of three parameters: the linearity of the sFIDA readout as a function of applied Aβ-SiNaP concentration, the coefficient of variation as well as the limit of detection.

The highest linearity for mean Pearson's correlation coefficient ρ of 0.94 was calculated for Aβ-SiNaPs spiked in EDTA plasma followed by heparin (ρ=0.94) and citrate (ρ=0.37) plasma. The lowest mean CV of 28% was obtained for EDTA followed by citrate (CV=39%) and heparin plasma (CV=67%). The lowest LOD of 16 fM was obtained for quantitation of Aβ-SiNaPs spiked in EDTA plasma followed by LOD of 19 fM and 34 fM for citrate and heparin plasma, respectively.

EDTA, citrate and heparin are the most common anticoagulants for blood plasma treatment in clinical practice. Whereas the anticoagulative effect of EDTA and citrate is attributed to the prevention of thrombin formation by chelating calcium required for the blood clotting cascade (Davie and Ratnoff, 1964), heparin functions by activating antithrombin (Olson and Chuang, 2002). Apart from this, heparin is known to bind to a variety of proteins including proteases, growth factors, chemokines, lipid binding proteins and adhesion proteins as summarized in Capila and Linhardt (2002) and thus might modulate matrix effects significantly by affecting the biochemical constitution of blood plasma. Moreover, it has been shown in several studies that heparin binds directly to Aβ species (Watson *et al.*, 1997; Madine *et al.*, 2012; Nguyen and Rabenstein, 2016) possibly interfering with Aβ oligomer quantitation and accounting for the attenuating effects in sFIDA assay presented here.

Altogether, this is in line with studies on quantitation of total Aβ levels from blood plasma. Vanderstichele *et al.* (2002) reported that plasma collected in citrate and heparin tubes did not result in any measurable Aβ levels, whereas Aβ levels in EDTA plasma could be readily detected (Vanderstichele *et al.*, 2000). Lachno *et al.* (2009) determined total Aβ levels in serum, EDTA, citrate, heparin and fluoride plasma with highest Aβ levels in EDTA treated plasma (Lachno *et al.*, 2009).

The well-described binding of Aβ to various plasma proteins (Koudinov *et al.*, 1994; Biere *et al.*, 1996; Koudinov *et al.*, 1998) might lead to a masking of epitopes and ultimately result

in signal attenuation due to impaired capturing and probe detection. Previously, an interaction between prion protein aggregates and low density lipoproteins has been reported, making pretreatment with lipases and detergents necessary to counteract signal loss in sFIDA measurements (Safar *et al.*, 2006; Bannach *et al.*, 2012). In the present study, however, the presence of EDTA plasma did not have any adverse effect on detection and quantitation of Aβ-SiNaP down to the low femtomolar range.

The achieved coefficient of variation of 28% is a severe issue for further improvement. Also, more validation parameters as suggested by Andreasson *et al.* (2015) (Andreasson *et al.*, 2015) need to be addressed in future.

We conclude that EDTA is the most suitable anticoagulant for Aβ-SiNaP quantitation in blood plasma using the sFIDA assay. We therefore suggest that plasma samples for AD diagnosis in the sFIDA assay should be collected in EDTA tubes to ensure most accurate determination of Aβ oligomer levels in human blood plasma. Future investigations, however, will reveal, whether humans do contain detectable amounts of Aβ oligomers and whether they correlate with disease progression or prognosis. Thus, further work will focus on sFIDA measurements of clinical EDTA plasma samples from AD patients and controls in order to assess if Aβ oligomers can be exploited as a blood-based biomarker for AD.

Materials and methods

Plasma samples

A total of 15 blood plasma samples from 5 healthy donors were purchased from ZenBio, Inc. (BioCat GmbH, Heidelberg, Germany). Plasma samples were collected in BD Vacutainer tubes containing 12.15 mg K_2EDTA per 7.0 ml sample, 158 USP Units Heparin per 10.0 ml sample or 1 ml acid-citrate-dextrose solution B (4.8 g/l citric acid; 13.2 g/l Na_3Citrate; 14.7 g/l dextrose) per 6 ml sample, respectively. To avoid repeated freeze/thaw cycles, plasma samples were directly aliquoted and stored at -80°C until usage. Prior to aliquoting, plasma samples were centrifuged for 10 min at 20 000 *g* and the supernatant was preserved.

Silica nanoparticles coated with $A\beta_{1-42}$ (Aβ-SiNaPs)

Aβ-SiNaPs were prepared as described previously (Hülsemann *et al.*, 2016). Briefly, bare silica nanoparticles (SiNaPs) were synthesized via Stöber process and silanized with APTES to cover the surface with primary amino groups. Subsequent reaction with succinic anhydrid resulted in carboxylated SiNaPs, which were activated by EDC/NHS for covalent coupling of $A\beta_{1-42}$. The same batch of Aβ-SiNaPs was used for all spiking experiments to ensure equal size (diameter of approx. 30 nm) of the particles and Aβ distribution on the surface. 1 nM Aβ-SiNaP stock solution was serially diluted to 100 pM, 10 pM, 1 pM, 100 fM and 10 fM in plasma samples and PBS.

sFIDA protocol

For sFIDA assay a 384-well multititer plate (SensoPlate plus, Greiner Bio-One International, Frickenhausen, Germany) was used. All of the protocol steps were carried out under the clean bench to avoid dust and microbial contamination. Prior to functionalization of the glass surface, wells were cleaned with sodium hydroxide and hydrochloric acid. 5 M NaOH (Carl Roth, Karlsruhe, Germany) was applied for 15 min to the wells (95 µl/well) followed by three washing steps with the same volume of water. Immediately, 1 M HCl (32%, AnalaR NORMAPUR, VWR Chemicals, France) was incubated for 15 min in the wells (95 µl/well) followed by three washing steps with water and two washing steps with 70% ethanol (AnalaR NORMAPUR, VWR Chemicals, France). Shortly after wells dried at room temperature (RT), 45 µl of a DMSO (Sigma-Aldrich, Steinheim, Germany) ethanolamine mixture (Sigma-Aldrich, Steinheim, Germany) (v/v 2:3) was added to the wells and incubated overnight at RT. Afterwards, the wells were washed twice with DMSO and twice with 95 µl/well 70% ethanol and let dry. In the meantime, NHS-PEG-COOH (MW 5000, Laysan Bio, USA) was solved at 70°C in DMSO and cooled down to RT. 15 µl of 2 mM PEG solution were applied per well for 1 h followed by three washing steps with water. Activation of the PEG carboxyl groups was then performed by applying 30 µl/well of 100 mM EDC (Fluka, Buchs, Switzerland) and 100 mM NHS (Aldrich, Milwaukee, USA) mixture (v/v 1:1) in 0.1 M MES (Carl ROTH, Karlsruhe, Germany) buffer (pH 3.5) for 30 min. After washing the wells three times quickly with MES buffer, 15 µl/well capture antibody was added immediately for 1 h to the wells. As capture antibody, monoclonal anti-β-amyloid antibody NAB228 (Sigma-Aldrich, Steinheim, Germany) was diluted in PBS (Dulbecco's phosphate buffered saline 10×, Sigma-Aldrich, Steinheim, Germany) to a final concentration of 10 ng/µl and

centrifuged at 15 000 *g* for 10 min to remove the unsoluble components. Hereafter, the wells were washed twice with PBS-T (PBS + 0.05% Tween-20, Sigma-Aldrich, Steinheim, Germany) and twice with PBS. Next the surface was blocked with 50 µl/well Smart Block solution (Candor Bioscience, Wangen, Germany) followed by two washing steps with PBS-T and two steps with PBS. 15 µl/well sample was then applied to the surface and incubated overnight. Unbound sample components were removed by two washing steps with PBS-T and two washing steps with PBS. Finally, fluorescently labeled detection antibodies 6E10 Alexa Fluor 488 (Covance, Princeton, USA) and NAB228 Alexa Fluor 647 (Santa Cruz, Dallas, USA) were combined to the final concentration of 1.25 ng/µl each, centrifuged at 100 000 *g* for 1 h and applied to the wells (15 µl/well). After final washing twice with PBS-T and twice with PBS, wells were filled with 95 µl PBS.

Data acquisition

Acquisition of 14-bit grayscale images was performed using total internal reflection microscopy (AM TIRF MC, Leica Microsystems, Wetzlar, Germany). A total of 50 images per well (25 positions per channel) containing 1000 × 1000 pixels each were obtained for channel 0 (excitation at 635 nm, emission filter 705/72 nm) and channel 1 (excitation at 488 nm, emission filter 525/36 nm). The image size represents an area of 116 µm × 116 µm, thus in total 3.15% of the well surface (approx. 10 nm^2) were scanned. Laser intensity of 100%, exposure time between 1 s and 1.5 s and gain between 900 and 1000 were applied for image acquisition.

Artifact detection

Prior to data analysis, artificial images were removed from raw data pool applying two algorithms based on histogram analysis and cluster detection, respectively.

First, images were subjected to histogram artifact detection. This method is based on calculating the histogram for each image and counting the peaks by determination of local maxima in the histogram. Images with multimodal histograms (histograms containing more than one histogram maximum) were considered artificial and were excluded from further analysis. The image histogram was smoothed using 800 values for binning to eliminate background noise and thus avoid detection of local maxima. Via numerical differentiation the derivative of the smoothed histogram was calculated, which was then smoothed in the same way as the original histogram. After smoothing procedures, some rest noise can still cause

local maxima especially at points where function overlaps with x-axis. In order to determine the parameters for exclusion of images based on their histogram, a threshold was defined which includes two components: α and β. α is the number of pixels which form a maximum, β is a number of pixels which form a minimum. Only if α and β of adjacent maximum and minimum are high enough to meet α and β limits, a maximum was treated as a maximum. α limit of 400 and β limit of 300 were chosen as parameters for maxima determination.

Second, images with unimodal histograms (histograms with a single maximum) can still contain artifacts in form of large and/or bright spots. To detect these spots a cluster detection algorithm was applied to the images. This method is based on finding of agglomerations of pixels with intensities above a certain threshold. Depending on such parameters as cluster size, mean pixel intensity and standard deviation within a cluster, bright spots are identified as artifacts. Obtained grayscale images were transformed into binary images. The grayscale values with intensities ≤ mean grayscale value plus one standard deviation were set to 0, all others to 1. Using a rectangular structuring element with the size of 15 pixels × 15 pixels the images were eroded to identify large clusters and eliminate the small ones which represent Aβ-SiNaPs. To compensate pixel loss caused by erosion, dilation was applied to eroded images using the same structuring element.

An image was considered artificial and was excluded from further analysis, if at least one cluster fulfilled one of the following criteria: mean pixel intensity of more than 3000, a standard deviation of pixel intensity of more then 2800 or skewness of less than 0.

Data analysis

sFIDA readout

For data analysis of non-artificial images only a region of interest (ROI) consisting of the central 700 pixels × 700 pixels (corresponding to 490 000 pixels per image in total) was chosen in order to minimize the effects of inhomogeneous illumination of edge regions in TIRF microscopy images.

To reduce background noise, cutoffs were determined individually for each plasma sample based on the non-spiked control. This approach accounts for donor-specific background or signal by native Aβ oligomers which may influence the readout. For Aβ-SiNaPs diluted in PBS, the cutoff was determined from PBS control. The cutoff values for each channel were

determined as the intensity, which was exceeded by 1% of total pixels. Number of colocalized pixels from both channels above the respective cutoff is in following referred to as sFIDA readout.

The effects of different anticoagulants in plasma on sFIDA readouts were studied according to the criteria described below.

Linearity of the sFIDA readout

Pearson's correlation coefficient

Pearson's correlation coefficient (ρ) was calculated with MATLAB software as a criterion for linearity of the correlation between applied concentrations of Aβ-SiNaPs and obtained sFIDA readouts according to the formula:

$$\rho = \frac{N\sum xy - \sum x \sum y}{\sqrt{[N\sum x^2 - (\sum x)^2][N\sum y^2 - (\sum y)^2]}}$$

Where x is concentration of Aβ-SiNaPs, γ is the sFIDA readout and N is the number of x,γ pairs. Prior to mean value calculation, Olkin & Pratt correction was performed on Pearson's correlation coefficients (Olkin and Pratt, 1958; Eid *et al.*, 2013). Briefly, ρ was transformed to G_i according to the formula:

$$G_i = \rho_i \left(1 + \frac{1 - \rho_i^2}{2(n_i - 1 - 3)}\right)$$

where n is the number of samples in study i. Next, the weighted mean of G_i values was calculated for studies from $i = 1, \ldots, k$ according to the formula:

$$\bar{G} = \frac{\sum_{i=1}^{k} n_i G_i}{\sum_{i=1}^{k} n_i}$$

Thus, $\bar{G}$ is an estimator for mean correlation.

Test for linearity according to Mandel (Mandel's test)

The linearity of the sFIDA readout was further investigated using Mandel's fitting test (Mandel, 1964). This method provides evidence on linearity under consideration of the residual standard deviation for the first (linear) and second order (quadratic) calibration function. The H_0 hypothesis assumes no significant difference between the residual variances of the linear and quadratic calibration function. The Mandel's test was performed as follows (Funk *et al.*, 2005; Bruggemann *et al.*, 2006): The first and second order calibration functions are calculated including the residual standard deviations s_{y_1} and s_{y_2}:

$$s_{y_1} = \sqrt{\frac{\Sigma(y_i - \hat{y}_i)^2}{N-2}}, \text{ where } \hat{y}_i = a + bx_i$$

$$s_{y_2} = \sqrt{\frac{\Sigma(y_i - \hat{y}_i)^2}{N-3}}, \text{ where } \hat{y}_i = a + bx_i + cx_i^2$$

with:

y_i: observed sFIDA readout at each concentration level *i*

$\hat{y}_i$: estimation obtained from the respective regression analysis at *i*

N: total number of measurements

Next, the difference of the variances DS^2 is calculated based on the residual standard deviation s_{y_1} and s_{y_2}:

$$DS^2 = (N-2)s_{y_1}^2 - (N-3)s_{y_2}^2$$

Finally, the test value *PW* is calculated:

$$PW = \frac{DS^2}{s_{y_2}^2}$$

For the F-test, *PW* is compared with the corresponding value of the F-distribution $F_{crit;99\%(f_1,f_2,\alpha)}$, with $f_1 = 1$ and $f_2 = N - 3$ degrees of freedom at the significance level $\alpha = 0.01$.

For $PW < F_{crit;99\%}$ H_0 is accepted. The second order calibration function will not provide a significantly better fit; the calibration function of choice is linear.

For $PW > F_{crit;99\%}$ H_0 is retained, which indicates non-linearity (Bruggemann *et al.*, 2006).

Lack-of-fit test

The Lack-of-fit test (Massart, 1997) is performed by comparing the ratio of the error due to lack of fit of the respective calibration function and the error due to pure error obtained from replicative measurements with $F_{crit;99\%}$ at (k-2) and (n-k) degrees of freedom at the significance level $\alpha = 0.01$. The H_0 hypothesis assumes no lack of fit.

The Lack-of-fit test is calculated as follows: first, the sum of squares due to pure error and due to lack of fit are calculated, respectively:

$$SS_{PE} = \sum_{i}^{k} \sum_{j}^{n_i} (y_{ij} - \bar{y}_i)^2$$

$$SS_{LOF} = \sum_{i}^{k} n_i (\bar{y}_i - \hat{y}_i)^2$$

with:

i: concentration level, *k*: number of all concentration levels, *n*: number of replicates, $\bar{y}_i$: arithmetic mean of all observed values at *i*, $\hat{y}_i$: estimation obtained from the respective regression analysis at *i*. Next, the mean squares are calculated by dividing the sum of squares by the corresponding degrees of freedom (Massart, 1997).

$$MS_{LOF} = \frac{SS_{LOF}}{df}$$

$$MS_{PE} = \frac{SS_{PE}}{df}$$

For the F-test, the test value *LOF* is calculated as the arithmetic mean of both mean squares:

$$LOF = \frac{MS_{LOF}}{MS_{PE}}$$

For $LOF < F_{crit,99\%}$ H_0 is accepted. There is no lack of fit. For $LOF > F_{crit,99\%}$ H_0 is rejected. Saturated images for which sFIDA readout reached the maximum value of 490 000 (100 pM and 10 pM Aβ-SiNaPs in EDTA plasma as well as 100 pM Aβ-SiNaPs in PBS) were excluded from this analysis.

Coefficient of variation

Coefficient of variation (CV) was calculated as a criterion for intra-assay precision using Excel software. CV was calculated for each three replicate measurements for each standard concentration and negative control. The mean for each donor and each diluent was plotted using MATLAB software. Saturated images for 100 pM and 10 pM Aβ-SiNaPs in EDTA plasma as well as 100 pM Aβ-SiNaPs in PBS were excluded from this analysis.

Limit of detection

Limit of detection (LOD) was used as a criterion for sensitivity of the sFIDA assay. LOD was calculated as the mean from sFIDA readout for 6-fold replicate measurements of negative control (neg. control) from 5 individual donors (30 negative controls in total) and respective standard deviation (σ) according to the formula:

$$LOD = \text{sFIDA readout}_{(\text{neg. control})} + 3\sigma$$

Linear calibration curves for the correlation between concentrations of Aβ-SiNaPs and sFIDA readout for LOD determination were calculated with MATLAB software. Only values within the linear range of the obtained data were included for calculating the linear calibration curves (concentrations of 10 fM, 100 fM and 1 pM for all donors and anticoagulants). Using these calibration curves, the sFIDA readouts were correlated to their respective concentration.

Acknowledgements

This work was supported by the Federal Ministry of Education and Research within the projects "Validierung des Innovationspotenzials wissenschaftlicher Forschung - VIP" (03V0641), “Kompetenznetz Degenerative Demenzen” (01GI1010A), and the JPND “Neurodegenerative Disease Research/Biomarkers for Alzheimer’s and Parkinson’s disease” (01ED1203H), as well as the Michael J. Fox Foundation for Parkinson’s Research (11084).

References

Andreasson, U., A. Perret-Liaudet, L. J. van Waalwijk van Doorn, K. Blennow, D. Chiasserini, S. Engelborghs, T. Fladby, S. Genc*, et al.* (2015). A practical guide to immunoassay method validation. Front Neurol *6*, 179.

Banks, R. E., A. J. Stanley, D. A. Cairns, J. H. Barrett, P. Clarke, D. Thompson and P. J. Selby (2005). Influences of blood sample processing on low-molecular-weight proteome identified by surface-enhanced laser desorption/ionization mass spectrometry. Clin Chem *51*, 1637-1649.

Bannach, O., E. Birkmann, E. Reinartz, K. E. Jaeger, J. P. Langeveld, R. G. Rohwer, L. Gregori, L. A. Terry*, et al.* (2012). Detection of prion protein particles in blood plasma of scrapie infected sheep. PLoS One *7*, e36620.

Biere, A. L., B. Ostaszewski, E. R. Stimson, B. T. Hyman, J. E. Maggio and D. J. Selkoe (1996). Amyloid beta-peptide is transported on lipoproteins and albumin in human plasma. J Biol Chem *271*, 32916-32922.

Birkmann, E., F. Henke, N. Weinmann, C. Dumpitak, M. Groschup, A. Funke, D. Willbold and D. Riesner (2007). Counting of single prion particles bound to a capture-antibody surface (surface-FIDA). Vet Microbiol *123*, 294-304.

Birkmann, E., O. Schafer, N. Weinmann, C. Dumpitak, M. Beekes, R. Jackman, L. Thorne and D. Riesner (2006). Detection of prion particles in samples of BSE and scrapie by fluorescence correlation spectroscopy without proteinase K digestion. Biol Chem *387*, 95-102.

Blennow, K. (2004). CSF biomarkers for mild cognitive impairment. J Intern Med *256*, 224-234.

Blennow, K., N. Mattsson, M. Scholl, O. Hansson and H. Zetterberg (2015). Amyloid biomarkers in Alzheimer's disease. Trends Pharmacol Sci *36*, 297-309.

Bruggemann, L., W. Quapp and R. Wennrich (2006). Test for non-linearity concerning linear calibrated chemical measurements. Accreditation and Quality Assurance *11*, 625-631.

Capila, I. and R. J. Linhardt (2002). Heparin-protein interactions. Angew Chem Int Ed Engl *41*, 391-412.

Chuang, C. K., S. P. Lin, Y. T. Lin and F. Y. Huang (1998). Effects of anticoagulants in amino acid analysis: comparisons of heparin, EDTA, and sodium citrate in vacutainer tubes for plasma preparation. Clin Chem *44*, 1052-1056.

Davie, E. W. and O. D. Ratnoff (1964). Waterfall Sequence for Intrinsic Blood Clotting. Science *145*, 1310-1312.

Eid, M., M. Gollwitzer and M. Schmitt (2013). Statistik und Forschungsmethoden Lehrbuch; mit Online-Materialien. Weinheim, Wiley-VCH.

Fendl, B., R. Weiss, M. B. Fischer, A. Spittler and V. Weber (2016). Characterization of extracellular vesicles in whole blood: Influence of pre-analytical parameters and visualization of vesicle-cell interactions using imaging flow cytometry. Biochem Biophys Res Commun.

Funk, W., V. Dammann and G. Donnevert (2005). Qualitätssicherung in der Analytischen Chemie Anwendungen in der Umwelt-, Lebensmittel- und Werkstoffanalytik, Biotechnologie und Medizintechnik; Weinheim, Wiley-VCH.

Funke, S. A., E. Birkmann, F. Henke, P. Gortz, C. Lange-Asschenfeldt, D. Riesner and D. Willbold (2007). Single particle detection of Aβ aggregates associated with Alzheimer's disease. Biochem Biophys Res Commun *364*, 902-907.

Funke, S. A., L. Wang, E. Birkmann and D. Willbold (2010). Single-particle detection system for Aβ aggregates: adaptation of surface-fluorescence intensity distribution analysis to laser scanning microscopy. Rejuvenation Res *13*, 206-209.

Gerlach, R. F., J. A. Uzuelli, C. D. Souza-Tarla and J. E. Tanus-Santos (2005). Effect of anticoagulants on the determination of plasma matrix metalloproteinase (MMP)-2 and MMP-9 activities. Anal Biochem *344*, 147-149.

Haass, C. and D. J. Selkoe (2007). Soluble protein oligomers in neurodegeneration: lessons from the Alzheimer's amyloid β-peptide. Nat Rev Mol Cell Biol *8*, 101-112.

Hsieh, S. Y., R. K. Chen, Y. H. Pan and H. L. Lee (2006). Systematical evaluation of the effects of sample collection procedures on low-molecular-weight serum/plasma proteome profiling. Proteomics *6*, 3189-3198.

Hubbard, R. W., J. G. Chambers, A. Sanchez, R. Slocum and P. Lee (1988). Amino acid analysis of plasma: studies in sample preparation. J Chromatogr *431*, 163-169.

Hülsemann, M., C. Zafiu, K. Kühbach, N. Luhmann, Y. Herrmann, L. Peters, C. Linnartz, J. Willbold*, et al.* (2016). Biofunctionalized silica nanoparticles: standards in amyloid-β oligomer-based diagnosis of Alzheimer's disease. J Alzheimers Dis.

Jambunathan, K. and A. K. Galande (2014). Sample collection in clinical proteomics--proteolytic activity profile of serum and plasma. Proteomics Clin Appl *8*, 299-307.

Koudinov, A., E. Matsubara, B. Frangione and J. Ghiso (1994). The soluble form of Alzheimer's amyloid β protein is complexed to high density lipoprotein 3 and very high density lipoprotein in normal human plasma. Biochem Biophys Res Commun *205*, 1164-1171.

Koudinov, A. R., T. T. Berezov, A. Kumar and N. V. Koudinova (1998). Alzheimer's amyloid β interaction with normal human plasma high density lipoprotein: association with apolipoprotein and lipids. Clin Chim Acta *270*, 75-84.

Kühbach, K., M. Hülsemann, Y. Herrmann, K. Kravchenko, A. Kulawik, C. Linnartz, L. Peters, K. Wang*, et al.* (2016). Application of an amyloid β oligomer standard in the sFIDA assay. Front Neurosci *10*, 8.

Lachno, D. R., H. Vanderstichele, G. De Groote, V. Kostanjevecki, G. De Meyer, E. R. Siemers, M. B. Willey, J. S. Bourdage*, et al.* (2009). The influence of matrix type, diurnal rhythm and sample collection and processing on the measurement of plasma β-amyloid isoforms using the INNO-BIA plasma Aβ forms multiplex assay. J Nutr Health Aging *13*, 220-225.

Leidinger, P., C. Backes, S. Rheinheimer, A. Keller and E. Meese (2015). Towards clinical applications of blood-borne miRNA signatures: the influence of the anticoagulant EDTA on miRNA abundance. PLoS One *10*, e0143321.

Madine, J., M. J. Pandya, M. R. Hicks, A. Rodger, E. A. Yates, S. E. Radford and D. A. Middleton (2012). Site-specific identification of an Aβ fibril-heparin interaction site by using solid-state NMR spectroscopy. Angew Chem Int Ed Engl *51*, 13140-13143.

Mandel, J. (1964). The statistical analysis of experimental data. New York [u.a.], Wiley Interscience.

Massart, D. L. (1997). Handbook of chemometrics and qualimetrics Elektronische Ressource. Amsterdam, New York, Elsevier.

Nguyen, K. and D. L. Rabenstein (2016). Interaction of the heparin-binding consensus sequence of β-amyloid peptides with heparin and heparin-derived oligosaccharides. J Phys Chem B *120*, 2187-2197.

Olkin, I. and J. W. Pratt (1958). Unbiased Estimation of Certain Correlation Coefficients. 201-211.

Olson, S. T. and Y. J. Chuang (2002). Heparin activates antithrombin anticoagulant function by generating new interaction sites (exosites) for blood clotting proteinases. Trends Cardiovasc Med *12*, 331-338.

Parvy, P. R., J. I. Bardet and P. P. Kamoun (1983). EDTA in vacutainer tubes can interfere with plasma amino acid analysis. Clin Chem *29*, 735.

Ribeiro, A., T. Ritter, M. Griffin and R. Ceredig (2016). Development of a flow cytometry-based potency assay for measuring the *in vitro* immunomodulatory properties of mesenchymal stromal cells. Immunol Lett *177*: 38-46.

Riches, P., R. Gooding, B. C. Millar and A. W. Rowbottom (1992). Influence of collection and separation of blood samples on plasma IL-1, IL-6 and TNF-α concentrations. J Immunol Methods *153*, 125-131.

Safar, J. G., H. Wille, M. D. Geschwind, C. Deering, D. Latawiec, A. Serban, D. J. King, G. Legname*, et al.* (2006). Human prions and plasma lipoproteins. Proc Natl Acad Sci USA *103*, 11312-11317.

Sanagi, M. M., Z. Nasir, S. L. Ling, D. Hermawan, W. A. Ibrahim and A. A. Naim (2010). A practical approach for linearity assessment of calibration curves under the International Union of Pure and Applied Chemistry (IUPAC) guidelines for an in-house validation of method of analysis. J AOAC Int *93*, 1322-1330.

Selkoe, D. J. (1991). The molecular pathology of Alzheimer's disease. Neuron *6*, 487-498.

Van Loco, J., M. Elskens, C. Croux and H. Beernaert (2002). Linearity of calibration curves: use and misuse of the correlation coefficient. Accreditation and Quality Assurance *7*, 281-285.

Vanderstichele, H., E. Van Kerschaver, C. Hesse, P. Davidsson, M. A. Buyse, N. Andreasen, L. Minthon, A. Wallin*, et al.* (2000). Standardization of measurement of β-amyloid(1-42) in cerebrospinal fluid and plasma. Amyloid *7*, 245-258.

Wang-Dietrich, L., S. A. Funke, K. Kuhbach, K. Wang, A. Besmehn, S. Willbold, Y. Cinar, O. Bannach*, et al.* (2013). The amyloid-β oligomer count in cerebrospinal fluid is a biomarker for Alzheimer's disease. J Alzheimers Dis *34*, 985-994.

Watson, D. J., A. D. Lander and D. J. Selkoe (1997). Heparin-binding properties of the amyloidogenic peptides Aβ and amylin. Dependence on aggregation state and inhibition by Congo red. J Biol Chem *272*, 31617-31624.

Wimo, A., L. Jonsson, J. Bond, M. Prince, B. Winblad and I. Alzheimer Disease (2013). The worldwide economic impact of dementia 2010. Alzheimer's Dement *9*, 1-11 e13.

Tables and figures

Table 1 Analysis on linearity of sFIDA readout from Aβ-SiNaP dilution series.

	Pearson	Mandel's test		Lack-of-fit test (LRM)		Lack-of-fit test (QRM)	
	ρ	PW	F	LOF	F	LOF	F
EDTA 1	0.97	0.88	9.33	3.94	7.21	0.17	7.21
EDTA 2	0.98	1.16	10.04	6.35	8.02	0.12	8.02
EDTA 3	0.99	1.71	9.33	3.94	7.21	0.08	7.21
EDTA 4	0.78	0.13	9.33	3.17	7.21	2.33	7.21
EDTA 5	0.97	1.12	9.33	5.04	7.21	0.15	7.21
Citrate 1	0.1	138.29	8.28	52.22	4.89	1.88	4.89
Citrate 2	0.64	127.13	8.28	36.96	4.89	0.63	4.89
Citrate 3	0.19	204.31	8.28	56.76	4.89	0.34	4.89
Citrate 4	0.5	131.22	8.28	33.64	4.89	0.58	4.89
Citrate 5	0.42	69.77	8.28	21.01	4.89	0.86	4.89
Heparin 1	0.16	10.36	8.28	4.62	4.89	1.86	4.89
Heparin 2	0.87	46.14	8.28	11.79	4.89	5.80	4.89
Heparin 3	0.77	6.45	8.28	2.90	4.89	1.24	4.89
Heparin 4	0.70	3.92	8.28	2.36	4.89	1.58	4.89
Heparin 5	0.69	12.04	8.28	5.27	4.89	2.09	4.89
PBS 1	0.92	0.14	9.33	1.74	7.21	0.47	7.21
PBS 2	0.98	0.12	9.33	0.18	7.21	0.16	7.21
PBS 3	0.94	0.66	8.68	3.89	5.74	0.46	5.74

Pearson's correlation coefficient ρ, Mandel's test as well as Lack-of-fit test was calculated to analyze the linearity of sFIDA readout from SiNaP dilution series at a significance level of 99%. For the Mandel-test H_0 assumes no significant difference between the residual variances. For PW < F H_0 is accepted, the calibration function of choice is linear. For the

Lack-of-fit test H_0 assumes that the applied model is appropriate, lack of fit occurs at LOF > $F_{crit,99\%}$.

Table 2 Summary of analysis on the effect of different anitcoagulants on assay outcome parameters.

Anticoagulant	ρ	CV [%]	LOD [fM]
EDTA	0.94	28	16
citrate	0.37	39	19
heparin	0.64	67	34
PBS	0.94	51	27

The assay outcome was evaluated by means of three parameters: the linearity of the sFIDA readout as a function of applied Aβ-SiNaP concentration (mean Pearson's correlation coefficient ρ), the mean coefficient of variation (CV) as well as the mean limit of detection (LOD).

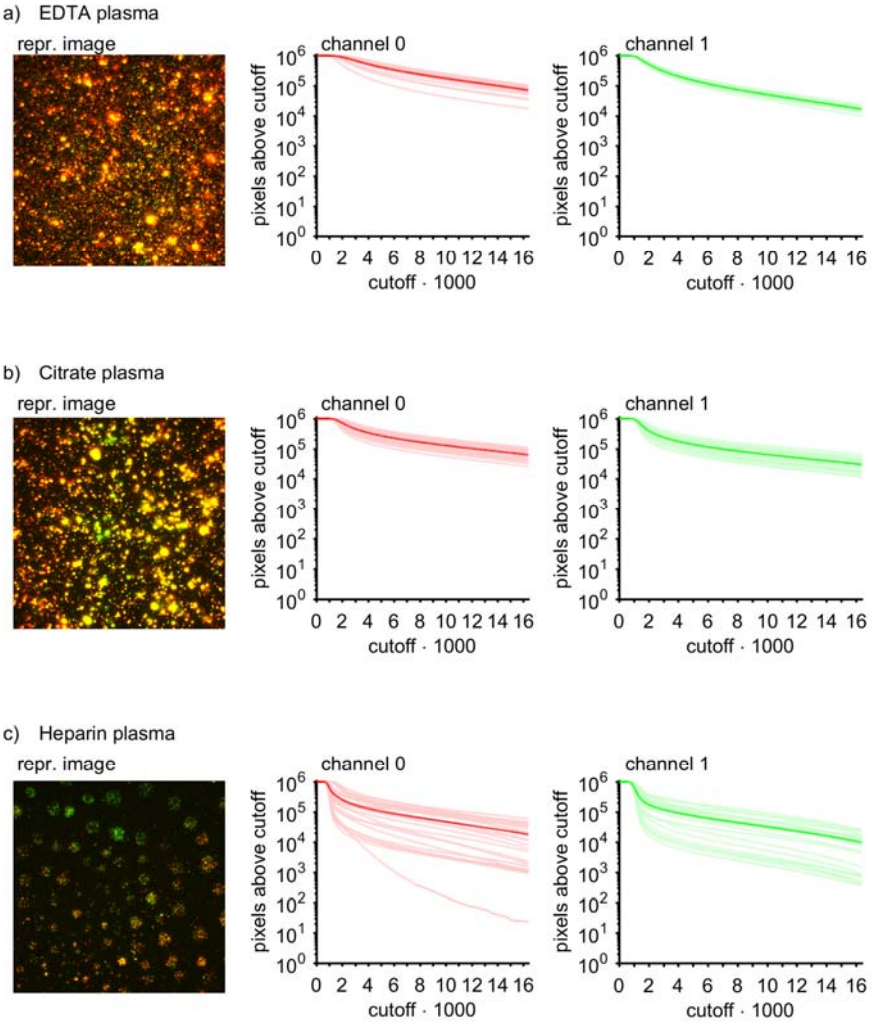

Figure 1 Representative images and cumulative histograms for 1 pM Aβ-SiNaP spiked in EDTA, citrate and heparin plasma.

1 pM Aβ-SiNaP was spiked in blood plasma treated with different anticoagulants from a single donor and subsequently applied to sFIDA assay. A representative image as a composition of channel 0 (exc.: 635 nm, em.: 705 nm) and channel 1 (exc.: 488 nm, em.: 525 nm) is given for (a) EDTA, (b) citrate and (c) heparin-treated plasma, respectively (left hand), as well as cumulative intensity histograms for channel 0 (middle) and channel 1 (right hand). Cumulative histograms for single images are depicted in light color whereas the mean cumulative histogram is depicted in dark color. The variation in intensity distribution between the images is higher for heparin compared to EDTA and citrate.

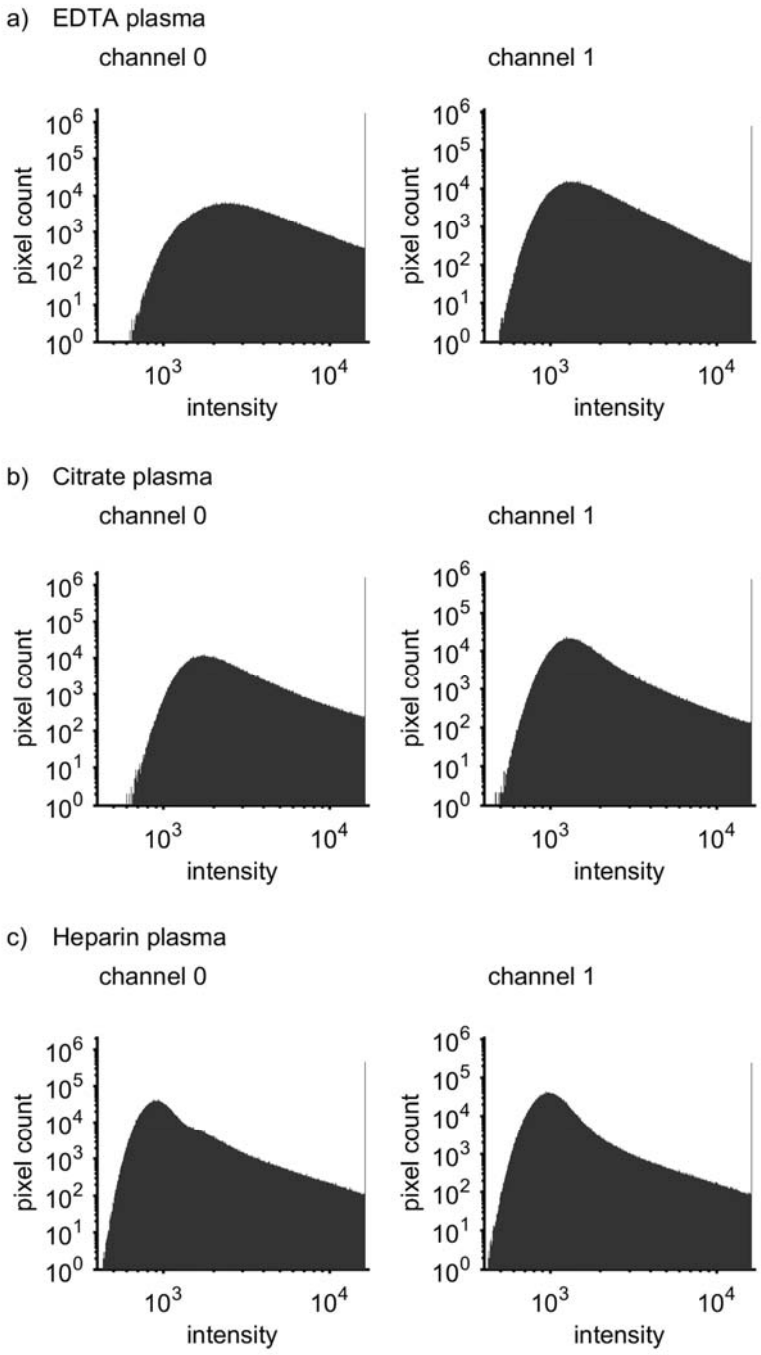

Figure 2 Intensity distribution for images obtained from 1 pM Aβ-SiNaPs spiked in EDTA, citrate and heparin plasma following sFIDA assay.

For channel 0 (exc.: 635 nm, em.: 705 nm) the major peak in intensity distribution for EDTA is approximately at 2400, for citrate at 1700 and for heparin plasma at 900 on a 14-bit grayscale, and for channel 1 (exc.: 488 nm, em.: 525 nm) at approximately 1300, 1300 and 1000, respectively. For channel 0 the major peak is approximately at 2400, for citrate at 1700 and for heparin plasma at 900 on a 14-bit grayscale, and for channel 1 at approximately 1300, 1300 and 1000, respectively.

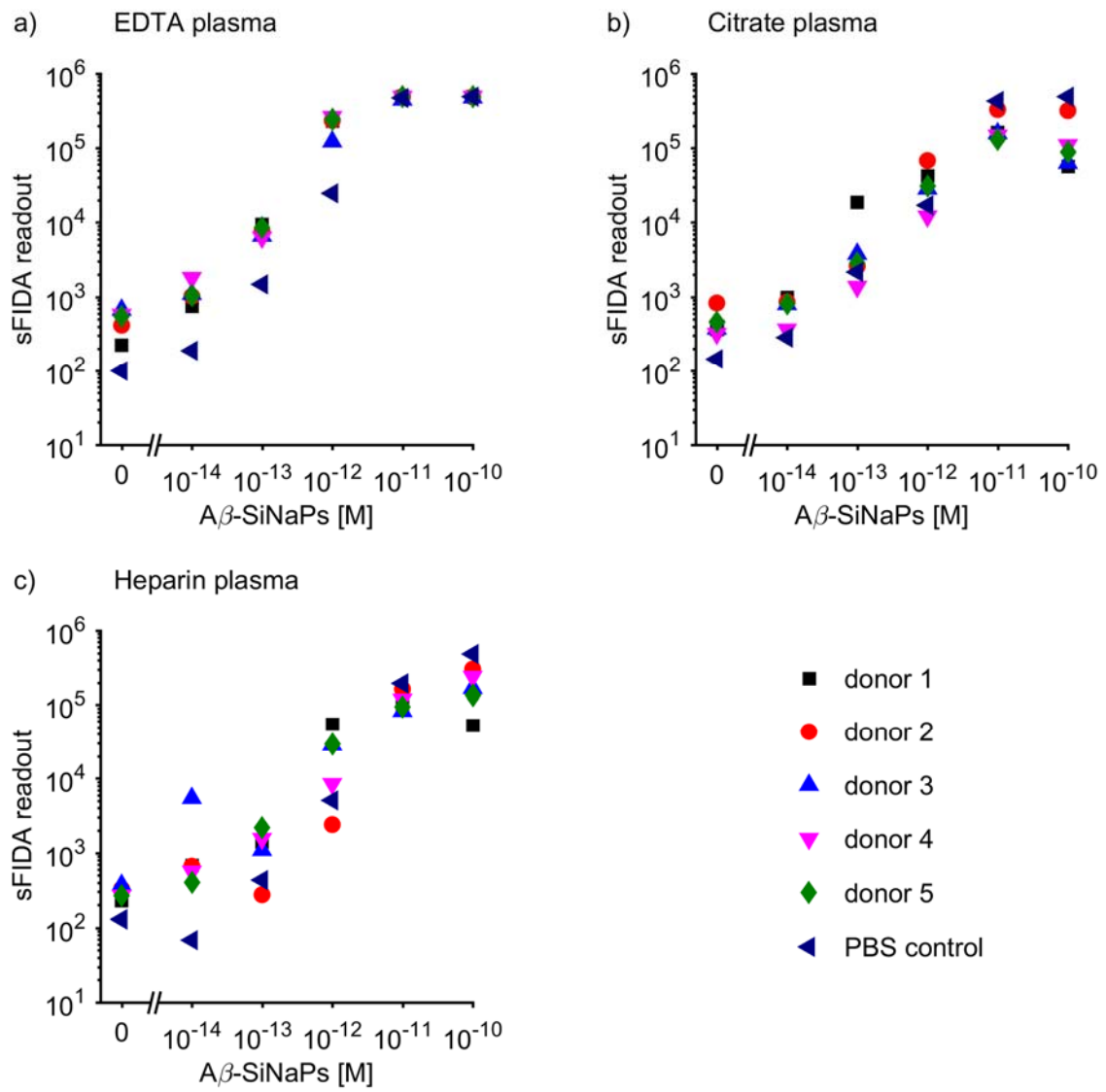

Figure 3 sFIDA readout for Aβ-SiNaPs spiked in EDTA, citrate and heparin plasma from five individual donors as well as in PBS.

Aβ-SiNaPs were serially diluted to 100 pM, 10 pM, 1 pM, 100 fM and 10 fM. As negative controls, non-spiked plasma samples were used (respective 0 M Aβ-SiNaP data points). Black rectangular symbols represent the sFIDA readout for donor 1, red circular symbols for donor 2, blue up-top triangular symbols for donor 3, magenta down-top triangular symbols for donor 4, green rhombical symbol for donor 5 and dark blue left-top triangular symbols for PBS control.

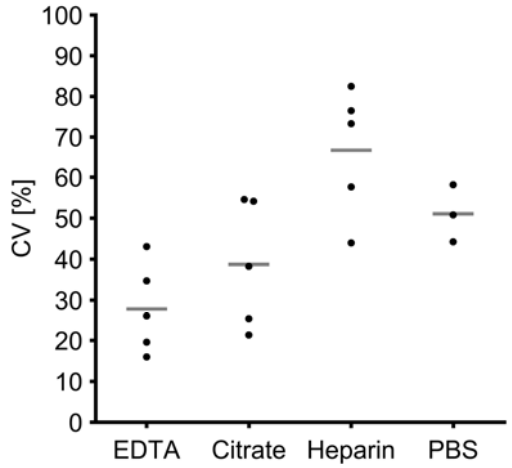

Figure 4 Coefficient of variation (CV) of sFIDA measurements for Aβ-SiNaPs diluted in EDTA, citrate and heparin plasma from five individual human donors.

The mean coefficient of variation (CV[%]) for the sFIDA readout was obtained for Aβ dilution series spiked in plasma samples from five different donors. The CV[%] was calculated as the standard deviation weighted by the mean sFIDA readout. The lowest and highest mean LOD is gained from EDTA and heparin treated blood plasma, respectively.

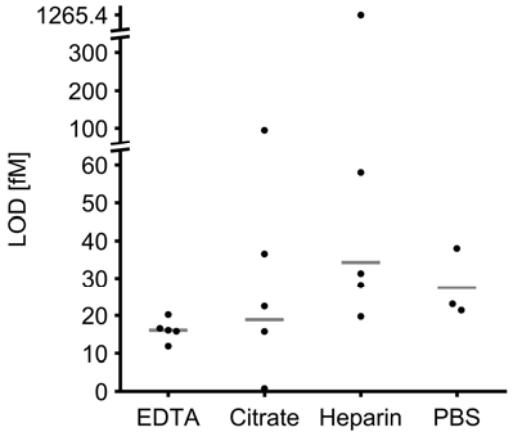

Figure 5 Limit of detection (LOD) from sFIDA measurements of Aβ-SiNaPs spiked in EDTA, citrate and heparin plasma from five donors as well as in PBS.

The mean limit of detection (LOD) for Aβ-SiNaPs spiked in blood plasma was obtained for six replicate measurements of each dilution series in samples from five different donors. The LOD was calculated from the sFIDA readout from the respective negative control plus three times the standard deviation. The lowest mean LOD of 16 fM was obtained for Aβ-SiNaPs spiked in EDTA plasma followed by 19 fM (incl. outlier: 34 fM) for citrate, 27 fM for PBS and 34 fM (incl. outlier: 280 fM) for heparin.